SECOND EUROPEAN CONFERENCE ON EARTHQUAKE ENGINEERING
AND SEISMOLOGY, ISTANBUL AUG. 25-29, 2014

DYNAMIC RESPONSE CHARACTERISTICS OF BUILDINGS SUBJECTED TO PULSE-LIKE GROUND MOTIONS

Yasuhiro HAYASHI[1], Rie OKAZAWA[2], Hiroshi YASUMOTO[3] and Hiroyuki MINAMI[4]

ABSTRACT

We have investigated the fundamental but very important response characteristics of buildings against the pulse-like ground motions which are predicted in the near-fault region of inland shallow earthquake. Especially, the soil structure interaction effects (SSI effects), contribution of each vibration mode, propagation of pulse-like wave in a building, and effects of viscous and hysteresis dampers are discussed in detail. In conclusion, the natural periods normalized by the pulse period T_p are very important characteristic values to evaluate the maximum response and building damage as well as the peak ground velocity or peak ground displacement.

INTRODUCTION

It is expected that destructive pulse-like ground motions are predicted to occur in the near-fault region of massive inland shallow earthquake and many tall buildings may suffer severe damage including collapse. However, uncertainty in estimating ground motion characteristics cannot be avoided. For example, Figure 1 shows the empirically obtained average relationships between the moment magnitude M_w and predominant period T_p observed in the near-fault regions. We call T_p as pulse period in this paper. In addition to the uncertainty of the moment magnitude of a predicted earthquake, uncertainty also exists in estimating the peak ground velocity V_p and pulse period T_p. As we discussed in this paper, these characteristic values of near-fault ground motions influence in the response of buildings strongly.

In this paper, we have clarified the response characteristics of buildings against the pulse-like ground motions. Sinusoidal pulse and Ricker wavelet are used for acceleration input wave to idealize the pulse-like ground motions. We have employed the peak velocity V_p and pulse period T_p as the characteristic values of pulse-like ground motions and used as analytical variables.

Two kinds of analysis models are used to evaluate the response characteristics of buildings. One analysis model is a sway-rocking model (SR model in Fig. 2) of buildings with spread foundation on the soil surface in order to consider the dynamic soil-structure interaction (SSI) effects. We investigate the variation in the response of soil and buildings when the predominant period of pulse-like ground motions T_p, the total height of building H and the average shear wave velocity of soil are parametrically changed.

[1] Professor, Kyoto university, Kyoto, Japan, hayashi@archi.kyoto-u.ac.jp
[2] Graduate student,Kyoto university, Kyoto, Japan, rp-okazawa@archi.kyoto-u.ac.jp
[3] Graduate student,Kyoto university, Kyoto, Japan, rp-yasumoto@archi.kyoto-u.ac.jp
[4] Engineer,Shimizu Corp., Tokyo, Japan, minami_h@shimz.co.jp

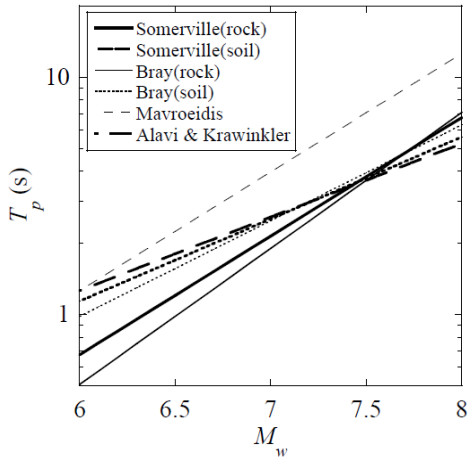

Figure 1. Relationship pulse period and moment magnitude

Another analysis model is an uniform transversely vibrating beam with a fixed and free ends with fundamental natural period T_1. First, the modal analysis is conducted analytically to investigate the contribution of vibration modes to the maximum drift angle R_{max}. The effects of the type of damper such as hysteretic damper or viscous damper on R_{max} are also studied. Next, linear and nonlinear response analyses are carried out to investigate the height H_m where the maximum drift angle has produced from the view point of pulse like deformation propagation through the building and its damage concentration.

SOIL-STRUCTURE INTERACTION EFFECTS

Building height is H=3.5N if the number of stories is N and story height is 3.5m. The foundation is a square, L=30m on a side, and is built on the semi-infinite soil with shear wave velocity V_s. The building-soil interaction system is modeled by a Sway Rocking model (SR model), as shown in Fig. 2.

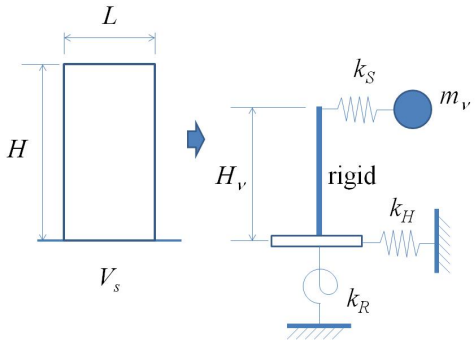

Figure 2. SR model considering SSI effects

Upperstructure is treated as an equivalent SDOF system, and its natural period T_0 with damping factor h_0 of 0.03 is given by Eq.(1) if foundation is fixed.

$$T_0=\alpha N \tag{1}$$

where proportional constant α=0.07. Weight per unit area is set to 1t/m^2, and massless rigid foundation is assumed. If acceleration of gravity is g, the total mass of a building will be $m=NL^2$/g. If the fundamental mode shape of the upperstructure is assumed to be linear, the equivalent mass m_v and the equivalent height H_v are given by

$$m_v=\frac{1.5(N+1)}{2N+1}m,\ H_v=\frac{2N+1}{3N}H. \tag{2}$$

The impedance functions of horizontal and rotational spring at the foundation are estimated based on the central displacement under uniform loading at the surface of the soil as follows.

$$k_H(\omega) = k_{H0} - \omega^2 m_{H0} + i\omega c_{H0}$$
$$k_R(\omega) = k_{R0} - \omega^2 m_{R0} + i\omega c_R(\omega)$$
$$k_{H0} = \frac{2\pi}{2-\nu} G r_H,\ m_{H0} = \frac{2\pi}{2-\nu}\frac{\Gamma_2^2}{12}\cdot\rho r_H^3,\ c_{H0} = \frac{2\pi}{2-\nu}\frac{\Gamma_2}{2}\rho V_s \cdot r_H^2 \quad (3)$$
$$k_{R0} = \frac{\pi}{2(1-\nu)} G r_R^3,\ m_{R0} = \frac{\pi}{2(1-\nu)}\frac{\Gamma_1^2}{6}\cdot\rho r_R^5,\ c_R(\omega) = \frac{\pi}{2(1-\nu)}\frac{\Gamma_1^3}{12}\frac{\rho}{V_s}\cdot r_R^6\omega^2,$$

where unit volume weight $\gamma=\rho g$=1.9 t/m^3, $G=\rho V_s^2$ and (ν, Γ_1, Γ_2)=(1/3, 1.212, 0.912). Moreover, r_H and r_R are the radius of a circle with equivalent cross-section area and second moment of area, respectively, to a square of one side L.

The u_G, u_{GH}, u_{GR}, and u_B denotes the ground displacement, relative horizontal displacement and rotational displacement of the foundation, and the deformation of the upperstructure, respectively. Displacement amplification ratio $|u_B/u_G|$ for V_s=100m/s and fixed foundation model (FIX) is shown in Fig. 3. In this figure, the natural frequency of the fixed foundation model is f_0 (=1/ T_0). By considering the SSI effects, equivalent natural period T_{e0} increases and is approximated by the following equation.

$$T_{e0} = T_0\sqrt{1+\frac{k_s}{k_{H0}}+\frac{k_s H_v^{\ 2}}{k_{R0}}} \quad (4)$$

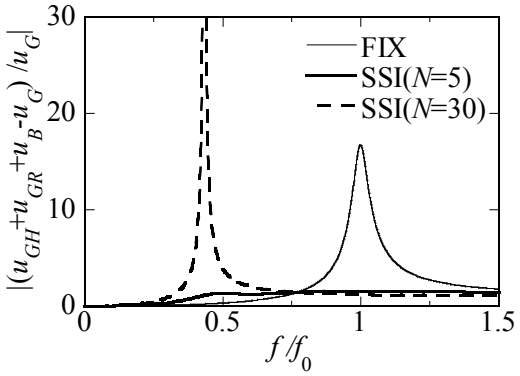

Figure 3. Transfer functions (V_s=100m/s)

Input ground motions

Sinusoidal pulses (Eq.(5)) or Ricker wavelets (Eq.(6)) is used for pulse type input ground motions as shown in Fig. 4.

$$\ddot{u}_G(t) = A_p \sin\omega_p t, \quad (5)$$

where $\omega_p = 2\pi/T_p$ and $A_p = \pi V_p / T_p$.

$$\ddot{u}_G(t) = A_p(\tau^2-1)\exp(-\tau^2/2), \quad (6)$$

where $\tau = \sqrt{2}\pi(t-T_p)/T_p$, $A_p = \sqrt{2e}\pi V_p / T_p$.

The T_p is pulse period, A_p and V_p are the peak acceleration and velocity, respectively.

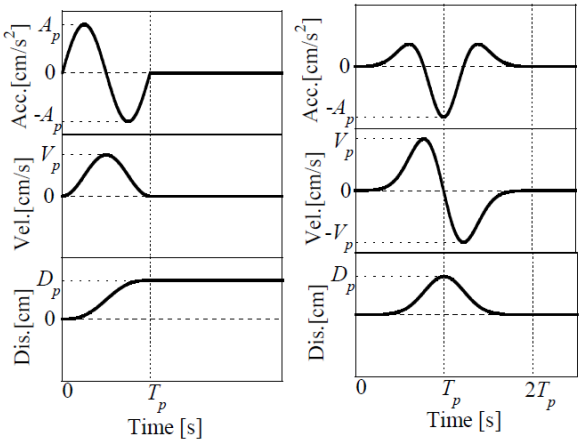

Figure 4. Input ground motions (left : sinusoidal pulse, right : Ricker wavelet)

Linear response analysis

Frequency response analysis is conducted and the linear response characteristics of SSI system under pulse type ground motions of V_p=100cm/s are investigated. The influence of SSI effects to the maximum response displacement $D_{\max}$ normalized by the peak ground motion D_p with pulse period T_p =1s is shown in Fig. 5. The difference of response between SR model and FIX model increases as V_s decreases. This tendency is evident in the low-rise building of N=5-10.

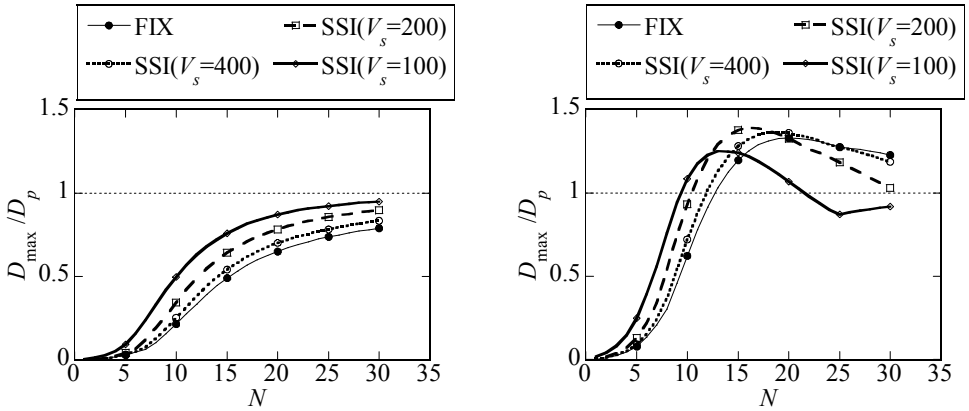

(a) Sinusoidal pulse (b) Ricker wavelet

Figure 5. Maximum displacement response (Influence of V_s, T_p =1s)

Then, Figure 6 shows the variation of $D_{\max}/D_p$ with pulse period T_p. The difference in the maximum response of SR model and FIX model varies with pulse period T_p and the number of stories N. It is thought that the difference may correspond to that in the fundamental natural period. Therefore, relationship between T_{e0}/T_p and $D_{\max}/D_p$ is shown in Fig. 7. Pulse type ground motions of T_p = 1s or 3s are input to buildings on the soil of V_s =400, 200, 100 m/s. Displacement response spectra for the damping ratio of 0.03 is also shown in the same figure. Results obtained using SR model agrees very well with normalized displacement response spectra.

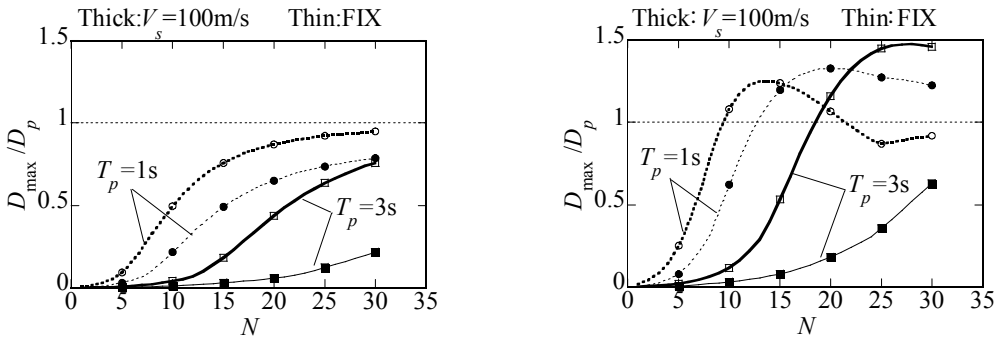

Figure 6. Maximum displacement response (Influence of T_p)

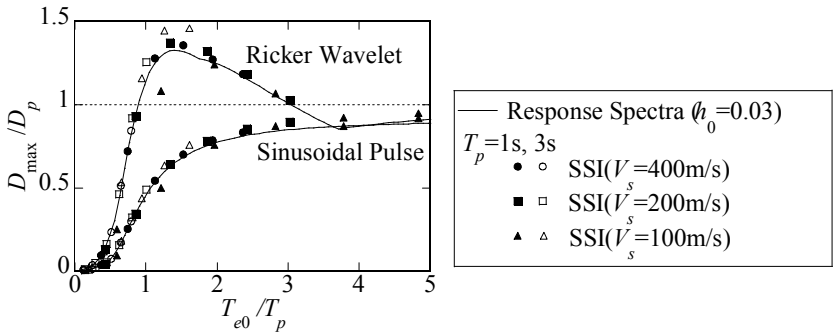

Figure 7. Normalized displacement response spectra (h_0=0.03) and maximum displacement response (Linear)

Nonlinear response analysis

In this subsection, influence of SSI effects is studied if the nonlinearity of buildings is taken into account. Let the restoring force characteristics of upperstructure be a trilinear type as shown in Fig. 8.

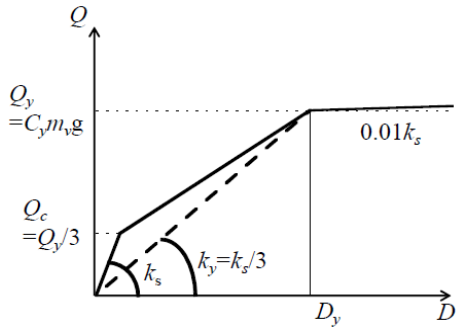

Figure 8. Restoring force characteristics

In this study, the yield base shear coefficient C_y is set to be in inverse proportion to the number of stories N.

$$C_y = \beta / N \tag{7}$$

If m_v and H_v are the effective mass and effective height of the building, R_y (=1/150) is the yield shear deformation angle, yield shear force Q_y and yield deformation D_y are expressed as follows.

$$Q_y = C_y m_v g \tag{8}$$

$$D_y = H_v R_y$$

Proportional constant β in Eq.(7) is related to α=0.07 in Eq.(1) as

$$\alpha = \sqrt{\frac{4\pi^2 d}{9g\gamma}\frac{2N+1}{N}} \cong 0.145/\sqrt{\beta} \tag{9}$$

Therefore, the results for β=3 (α=0.083) are shown in the following.

Figure 9 shows the relationship between T_{e0}/T_p and D_{max}/D_p obtained from nonlinear response analyses for SR (SSI) model and fixed foundation (FIX) model. In this figure, T_{e0} is the equivalent natural period of linear SSI system calculated from Eq.(4). For T_{e0}/T_p <1.5, normalized displacement response spectra underestimate the maximum response nonlinear response of buildings due to the underestimation of equivalent natural period. However, normalized displacement response spectra gives us a good estimation of the maximum displacement response for T_{e0}/T_p >1.5 because the maximum displacement response can be determined by the peak ground displacement D_p.

The maximum total response angles R_{max}= D_{max} /H_v and shear deformation angles of upperstructure R_{0max}= max(u_B)/H_v of linear SR model (SSI) and fixed foundation model (FIX) to sinusoidal pulse waves of T_p=1s are shown by thin lines in Fig. 10. The R_{max}=R_{0max} for the fixed foundation model.

It is pointed out that R_{max} increases by considering SSI effects because of the increase in equivalent natural period T_{e0}. However the shear deformation of upper structure R_{0max} itself slightly is smaller than R_{max} (FIX) for low-rise buildings (see N<10). On the other hand, increase in R_{max} by the SSI effects is not so large for N>15, but the reduction in R_{0max} becomes larger.

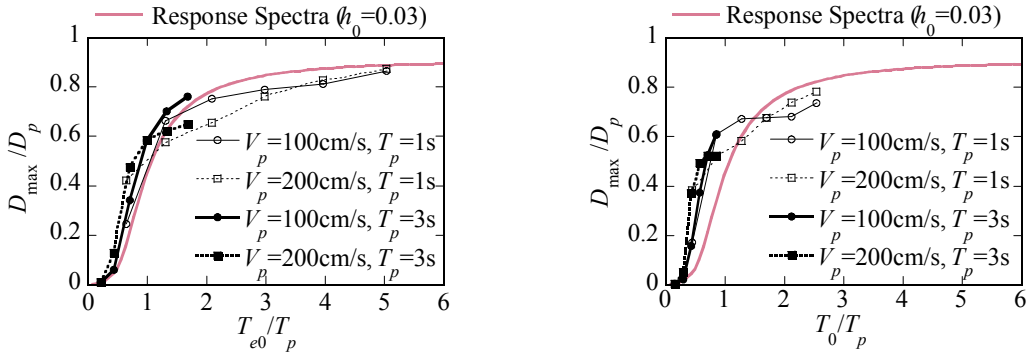

(a) SSI (b) FIX

Figure 9. Normalized displacement response spectra (h_0=0.03) and maximum displacement response (Nonlinear)

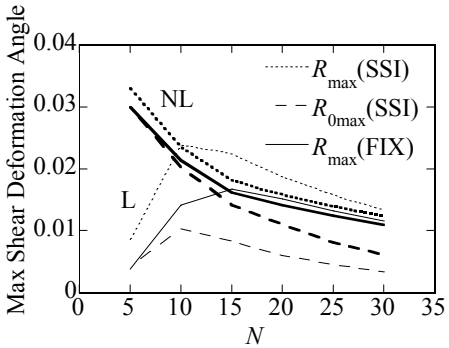

Figure 10. Maximum shear deformation angle for linear (L) and nonlinear (NL) soil-structure interaction analyses

The maximum response angle R_{max} and maximum shear deformation angle of upperstructure R_{0max} of nonlinear SSI systems to sinusoidal pulse waves is shown by bold lines in Fig. 10. It is pointed out that the SSI effects becomes smaller by considering the nonlinearity of buildings especially in R_{max}. In addition, R_{max} decreases with the number of stories. This is because the maximum displacement response D_{max} approaches by considering the nonlinearity of the upperstructure but equivalent height H_v increases with N.

When changing the peak ground velocity V_p with 100 or 200cm/s and the pulse period T_p with 1s, 2s, 3s, the R_{max} and R_{0max} are also shown in Fig. 11. As V_p increases, the difference of R_{max} for SR model and the fixed foundation model decreases. Namely, the SSI effects are not so large if V_p increases and the nonlinearity of upperstructure progresses.

If V_p is constant, the peak ground displacement D_p and the maximum response angle R_{max} for high-rise buildings increase with T_p. However, the maximum response angle R_{max} or R_{0max} drastically reduce if the number of stories N is less than a critical value N_c. For example, N_c=15 is for V_p=200cm/s and T_p =3s as shown in Fig.11(c). Then, N_c increases with T_p and contrarily decreases with V_p. This characterizes the damage tendency of buildings near the epicentral area. Therefore, when changing pulse period T_p, the height of buildings suffering damage may change drastically.

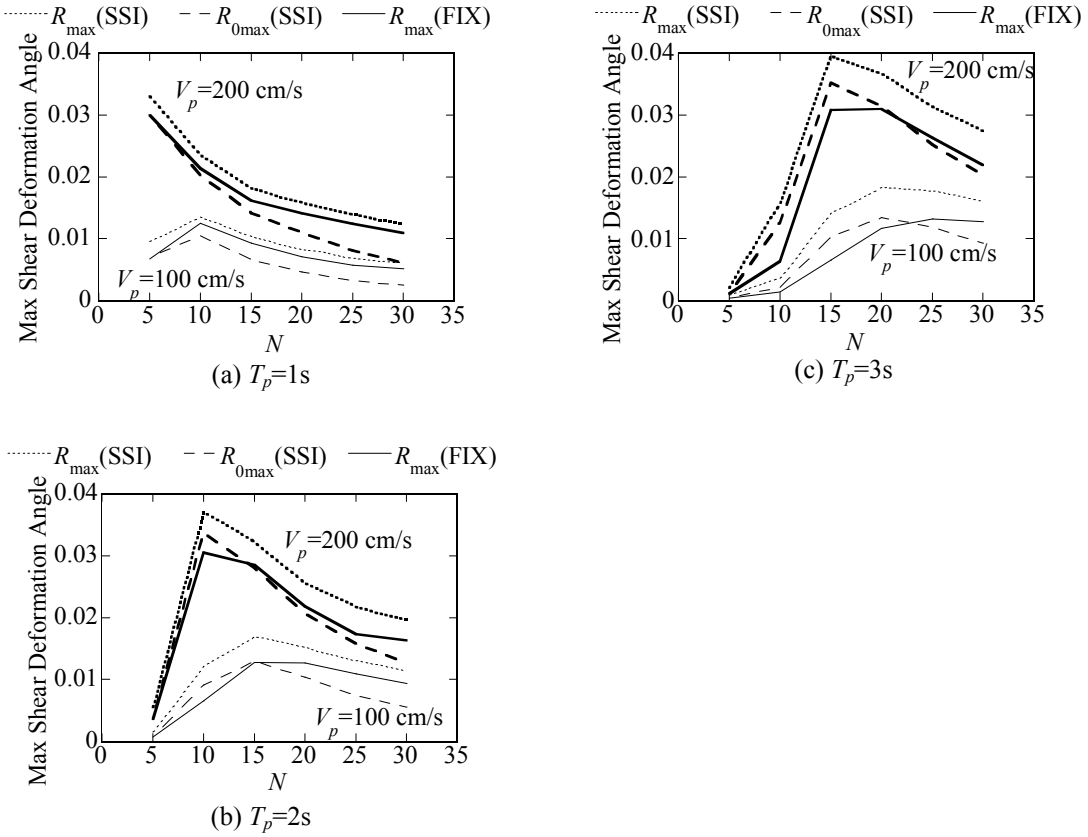

Figure 11. Maximum shear deformation angle considering nonlinear soil-structure interaction

MAXIMUM RESPONSE OF UNIFORM SHEAR-BEAM MODEL

In this section, buildings of height H fixed at the foundation is modeled by a uniform shear-beam model as shown in Fig. 12. We discuss the maximum response of the uniform shear-beam model subjected to Ricker wavelets.

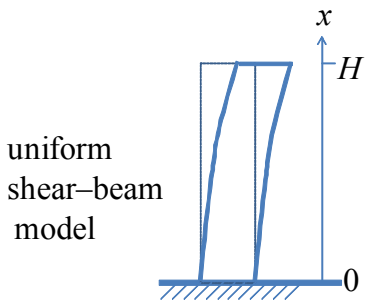

Figure 12. Uniform shear-beam model

Modal analysis of undamped system

First, the modal analysis is conducted analytically to investigate the contribution of vibration modes to the maximum drift angle R_{max}. In this subsection, we consider an undamped shear-beam model.
If the natural period T_1 of the fundamental mode is proportional to the height H as

$$T_1 = \alpha_1 H \tag{10}$$

the s-th natural period T_s is expressed as

$$T_s = T_1/(2s-1). \tag{11}$$

The natural mode $\phi_s(x)$ and its participation factor β_s are given as follows.

$$\phi_s(x) = \sin((2s-1)x\pi/2H) \tag{12}$$

$$\beta_s = 4/(2s-1)\pi \tag{13}$$

Here, $\psi_s(x)$ is called the drift angle mode in this paper and is obtained by normalizing the function obtained from the differentiation of the natural mode from height x.

$$\psi_s(x) = \cos((2s-1)x\pi/2H) \tag{14}$$

The maximum response of the s-th mode ${}_sR_{max}$ is given by using the displacement response spectra S_d as

$${}_sR_{max}(x) = \beta_s \cdot (d\phi_s(x)/dx) \cdot S_d({}_s\tau) \tag{15}$$

where ${}_s\tau$ is the normalized s-th mode natural period ${}_s\tau = T_s/T_p$. Above equation can be written as

$${}_sR_{max}(x) = {}_sR_{eff} \cdot \psi_s(x) \tag{16}$$

The ${}_sR_{eff}$ is the contribution of s-th mode to the maximum drift angle. If considering the wave propagation in infinite shear-beam, the maximum deformation angle R_{0max} can be easily obtained as follows.

$$R_{0max} = \alpha_1 V_p/4 \tag{17}$$

Then, using this value, ${}_sR_{eff}$ is normalized as

$$\frac{{}_sR_{eff}}{R_{0max}} = \frac{4\sqrt{2e}}{\pi} \cdot \frac{S_d({}_s\tau)}{{}_1\tau D_p}. \tag{18}$$

It is pointed out that the contribution of the first mode is dominant in the maximum drift angle if ${}_1\tau = T_1/T_p < 2$. In other words, contribution of higher mode cannot be negligible if $T_1/T_p > 2$. The ${}_sR_{eff}/R_{0max}$ is shown in Fig. 13.

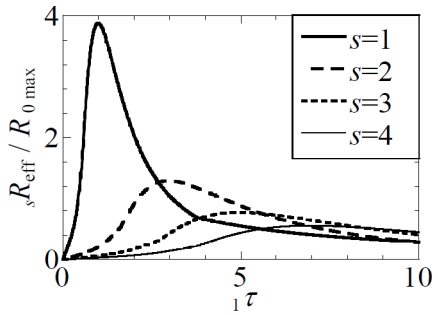

Figure 13. The contribution of s-th mode to the maximum drift angle

Wave propagation in undamped shear-beam

Next, wave propagation behavior in the undamped shear-beam is demonstrated. Shear-beam is modeled by using an equivalent lumped mass-spring system. Namely, mass and stiffness are constant. Assuming a building of 40 stories, the fundamental natural period T_1 is set to be 4.8s. In order to compare the contribution of higher mode, T_1/T_p is set to be 1.0 or 4.0 as shown in Fig. 14. By showing the waveform of shear drift angle at all floors, wave propagation behavior is investigated. If T_1/T_p=1.0, the building is shaking in the fundamental mode. However, if T_1/T_p=4.0, we cannot distinguish each mode but the propagation of a wavelet. Then, the maximum drift angle $_{\max}R_{\max}$ occur due to the interference of an upward wave from the bottom and a downward wave reflected at the top. Therefore, the maximum drift angle occur at a middle to upper floor if T_1/T_p is large.

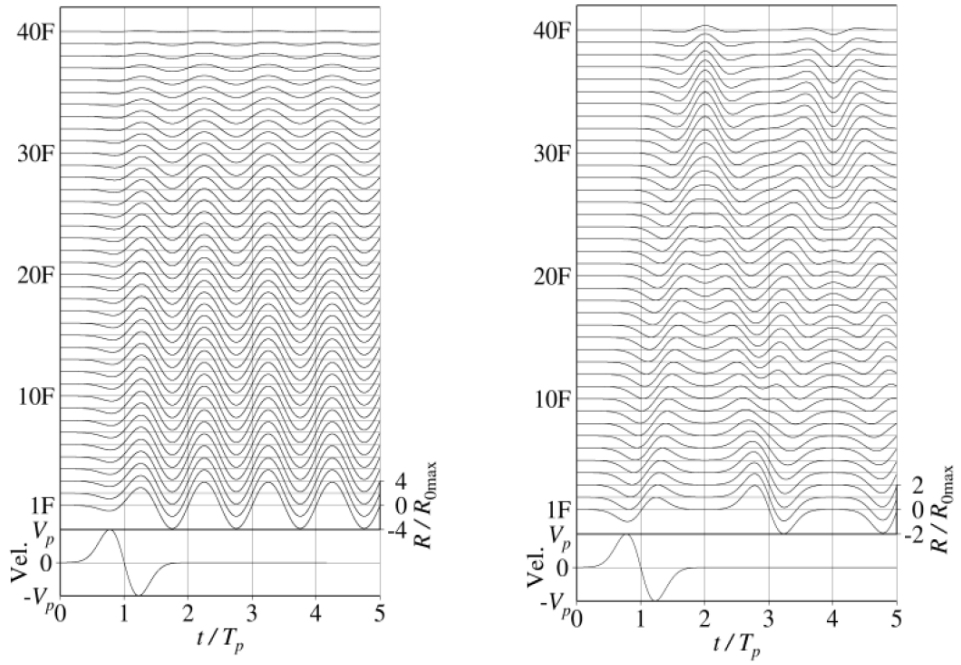

(a) T_1/T_p=1.0 (b) T_1/T_p=4.0

Figure 14. Propagation behavior of drift angle in buildings (T_1=4.8s)

The H_m and t_m are, respectively, the height and time of the maximum drift angle $_{\max}R_{\max}$ has produced. Figure 15 shows $_{\max}R_{\max}$, H_m, and t_m with respect to the non-dimensional fundamental natural period $_1\tau = T_1/T_p$. For $_1\tau > 2$, $_{\max}R_{\max}$, H_m, and t_m can be estimated as follows, respectively.

$$_{\max}R_{\max} / R_{0\max} = 2 \tag{19}$$

$$H_m / H = 1 - 1/ {}_1\tau \tag{20}$$

$$t_m / T_p = {}_1\tau / 4 + 1 \tag{21}$$

By using these equations, we can roughly estimate the maximum drift angle, height and time of occurrence.

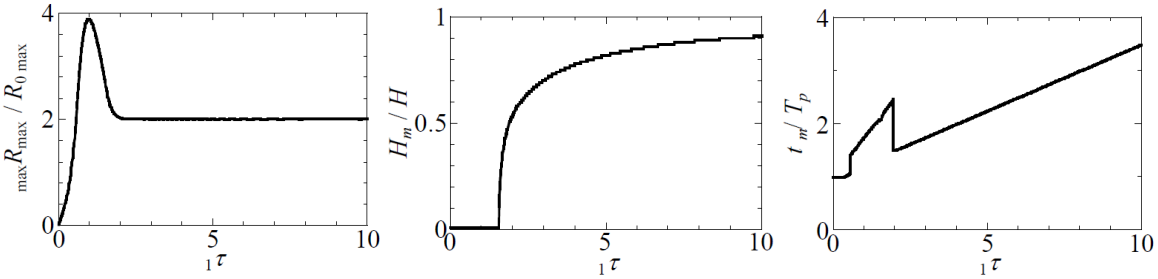

(a) Maximum response (b) Height of the maximum response occurrence (c) Time of the maximum response occurrence

Figure 15. Value, occurrence position, and occurrence time of maximum response

Maximum response and response reduction effects by dampers

Effects of the type of damper such as hysteretic dampers or viscous dampers on reduction in R_{max} are also studied. In addition, nonlinear time-domain analyses are carried out to investigate the height H_m where the maximum drift angle has produced from the view point of pulse like deformation propagating through the building.

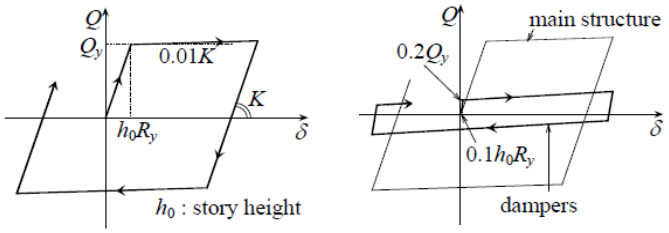

Figure 16. Restoring force characteristics of main structure (left) and hysteretic dampers (right)

In this subsection, nonlinear response analyses are carried out. Lumped mass system are used for building model. Then, mass, stiffness, and amount of dampers are uniform in the vertical direction. Ratio of mass and stiffness are determined to match the fundamental natural period T_1. Yield drift angle of the main structure R_y is set to be 1/150. Viscous dampers are installed so that the damping factor for fundamental natural period is 0.04. As for hysteretic dampers, on the other hand, the restoring force characteristics of dampers are bilinear type as shown in Fig. 16. The yield shear force of dampers are 0.2 times as large as that of main structure Q_y, while yield drift angle of the dampers are $0.1R_y$. Ricker wavelet whose V_p =100cm/s or 200cm/s is used for input ground motion.

The maximum drift angle are shown in Figs. 17 and 18. Results for the case of no damper and with dampers are shown in these figures.

First, height H_m of the maximum response occurrence is discussed for the case of no damper (see dashed lines in Fig. 17). For ${}_1\tau$ (=T_1/T_p)=1.2, H_m/H is 0, that is, the maximum drift angle occurred at the first floor regardless of V_p. As for ${}_1\tau$ =4.0, however, H_m/H is nearly equal to 0.7 for V_p =100cm/s, but H_m/H is 0 for V_p =200cm/s. Therefore, the H_m for nonlinear analysis depends on V_p as well as T_1/T_p. Especially, H_m suddenly shifts to the lower floor from the middle to upper floor as V_p increases if T_1/T_p>>1. The reason for this phenomenon is as follows. The H_m for linear model is shown in Fig. 15(b). Therefore, for small T_1/T_p, the maximum response always occur at the first floor. And for large T_1/T_p the maximum response occur upper intermediate story if the building is linear. However, deformation propagates from the bottom of the building just after the input of pulse-like ground

motions. Therefore, even if T_1/T_p is large enough, deformation concentrates gradually around the bottom of the building as V_p increases. Then, sudden shift of H_m to the lower floor from the middle to upper floor occurs as V_p increases.

Next, the reduction effects in the maximum response by dampers are discussed. The maximum response is reduced by viscous dampers regardless of V_p and reduction ratio of viscous damper becomes larger as ${}_1\tau = T_1/T_p$ increases as shown in Fig. 17. However, the maximum response for V_p =200cm/s and ${}_1\tau$ =1.2 slightly increases by installing hysteretic dampers as shown in Fig. 18(a). It is considered to be the reason for this that the equivalent natural period decreases by installing the hysteretic damper and approaches the peak period of displacement response spectra shown in Fig. 7.

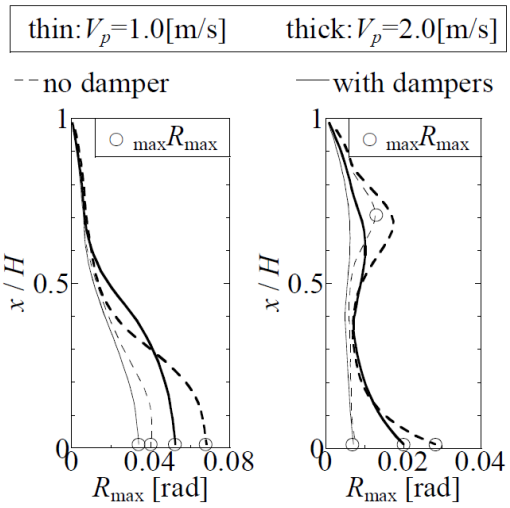

Figure 17. Maximum drift angle distribution (Viscous damper)

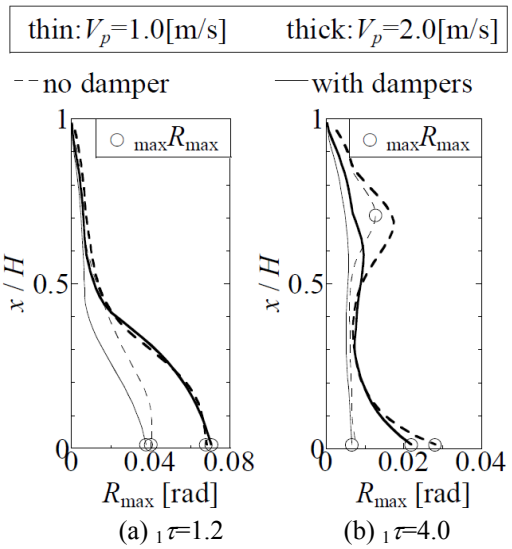

Figure 18. Maximum drift angle distribution (Hysteretic damper)

CONCLUSIONS

Based on our studies, we have pointed out very important response characteristics of buildings against the pulse-like ground motions as follows.

a. Results obtained using SR model agrees very well with normalized displacement response spectra. The linear soil-structure interaction effects is dependent on the ratio of equivalent natural period to pulse period T_{e0}/T_p.
b. The SSI effects are not so large if V_p increases and the nonlinearity of upperstructure progresses. If V_p is constant, the maximum drift angle for high-rise buildings increase with T_p. However, the maximum drift angle drastically reduce if the number of stories is less than a critical value. Therefore, when changing pulse period T_p, the height of buildings suffering severe damage may change drastically.
c. The maximum drift angle of linear tall buildings can be evaluated from V_p and T_1/T_p. Then, the occurrence time of the maximum response is also expressed by using T_1 and T_p. Next, the contribution of each vibration mode to R_{max} as well as the height H_m can be formulated using T_1/T_p.
d. The H_m for nonlinear analysis depends on V_p as well as T_1/T_p. Especially, H_m makes the sudden shift to the lower floor from the middle to upper floor as V_p increases if T_1/T_p>>1. This phenomenon can be understood using the theory of pulse propagation in an uniform transversely vibrating beam.
e. The maximum response is reduced by viscous dampers regardless of V_p and reduction ratio of viscous damper becomes larger as T_1/T_p increases. However, the maximum response for V_p =200cm/s and ${}_1\tau$ =1.2 slightly increases by installing hysteretic dampers. It is considered to be the reason for this that the equivalent natural period decreases by installing the hysteretic dampers

and approaches the peak period of displacement response spectra.

In conclusion, the natural periods normalized by the pulse period T_p are very important characteristic values to evaluate the maximum response and building damage as well as the peak ground velocity V_p or peak ground displacement D_p.

REFERENCES

G.P.Mavroeidis, A.S.Papageorgiou (2003) "A Mathematical Rep-resentation of Near-Fault Ground Motions", *Bulletin of the Seismological Society of America*, Vol. 93, No. 3, pp. 1099-1131, June.

P.G.Somerville (2003) "Magnitude Scaling of the Near Fault rup-ture directivity pulse", *Physics of the Earth and Planetary In-teriors*, 137, pp.201-212.

J.D.Bray, A.Rodriguez-Marek (2004) "Characterization of forward directivity ground motions in the near-fault re-gion", *Soil Dynamics and Earthquake Engineering*, 24, pp.815-828.

B.Alavi, H.Krawinkler (2000) "Consideration of near-fault ground motion effects in seismic design", *Proc. of 12th WCEE*, New Zealand.

H.Minami, Y.Hayashi (2013), "Response characteristics evalua-tion of elastic shear beam for pulse waves", *J. Struct. Constr. Eng.*, AIJ, Vol.77, No.675, 731-737 (in Japanese).